Internet of Things in Sport Training: Application of a Rowing Propulsion Monitoring System

Rémy Castro; Gabriel Mujica; Jorge Portilla

Internet of Things in Sport Training: Application of a Rowing Propulsion Monitoring System

Rémy Castro, Gabriel Mujica, *Member, IEEE,* and Jorge Portilla, *Senior Member, IEEE*

***Abstract*—The application of electronics, communication and telemetry technologies in the field of sport training is a major trend today, specially with the explosion of the Internet of Things paradigm. In particular, the rowing sport is one of the disciplines that could benefit from efficient, easy to integrate and low cost IoT technologies to help analysing and optimizing the performance of the rowers. However, traditionally monitoring tools in rowing are expensive and very limited. In this work a rowing propulsion monitoring system for on-board analysis of rower's key parameters is proposed, based on the development of a low-cost IoT device that combines sensing, global positioning, wireless communication and data fusion for runtime information processing and monitoring on the boat. A power calculation model during the stroke is also proposed in order to estimate the energetic efficiency of the strokes in relation with the boat velocity. An acceleration sensor on the oar is used to decompose the movement; a torsion sensor to calculate the rower's strength and energetic values; and navigation data for speed and distance values of the boat. A comprehensive comparative experimentation in a real rowing training scenario is performed, applying the proposed system and considering various rowers. Results show that the device provides a good vision in time of the movement and also very valuable technical information that can be used by rowers and trainers to define specific optimization profiles and improvement targets.**

***Index Terms*—Sport training, Internet of Things, wireless sensor networks, rowing, edge nodes.**

I. Introduction

The use of electronics, communication and computing technologies within sport applications and, in particular, to contribute to the monitoring and optimization of training in specific disciplines of sports is an increasingly important trend today. The applied technology is to be certainly combined with the expertise of athletes, to provide a more complete feedback based on both the obtained data from the training sessions and the experience of the subject under study. In addition to this, if the sport relies on the use of specific equipment, the implementation of technological systems to monitor and study the relationship between the athlete technique and the equipment behavior is a major concern to be analyzed.

One of the disciplines in which monitoring and analysing the performance of the athlete and its relationship with the involved technical equipment attracts significant attention is the rowing sport, where several elements are employed to carry out the sport, namely the shell with its foot stretcher, seat, oarlock and rigger, and the oars. Studying rowing techniques usually requires the study of various physic phenomena, and the rowing movement description can be complex. The literature about rowing is extensive and most of the existing works mainly focus on mechanics, bio mechanics, and fluid mechanics.

Optimizing the propulsion of a rowing boat usually takes place based on the experience of training with the help of advanced trainers. A rower obtains expertise with practice, during years of regular training. Moreover, specific technique improvements in a boat are noticed through the measurement of the rower (based on several available ways of static and dynamic analysis). However, the ultimate objective is to reach the highest possible speeds, which is a measurable parameter. In this way, there are works in the literature in which the authors define objectives functions in order to qualify the efficiency of the movement. In [1], the authors define the "Quality of the stroke" aiming to compare rower profiles with technical levels so as to give a tool for helping in improving the rowing technique. According to [2], there is nowadays a strong demand and curiosity from the athletes and the trainers for new technologies and, in particular, for IoT (Internet of Things) technologies [3, 4] in sport. They demonstrate that fine-grained monitoring in sport by using IoT tends to positively impact the technique of the athletes.

The rowing monitoring tools for rowing training exist but they are usually partial and intended to be for commercial purposes, or very complex and expensive for the experimental ones. As far as the authors know, there are no well-established commercial tools in the field that allow measuring at runtime and in a direct on-water way the power or the strength gave by the rower. Therefore, the main objective of this work is to design and implement an on-board propulsion monitoring system to provide the rower with useful parameters and improvement objectives in order to optimize his/her technique of rowing, by using IoT technologies. The main target is to develop a low-cost yet precise device to measure key parameters of the rowing training during the real-time session, that is, dynamic parameters at runtime, so that power and strength can be computed to further optimize the rower technique.

The design and implementation of the low-cost monitoring device for rowing movement is conceived such that it can be adjusted to different oars and rowing boats, that is, as less intrusive as possible. Based on the capabilities of the device, the aim is to obtain the speed, distance, and time measurements in real time and combined them with the information provided by the rower and the training conditions. Moreover, the frequency, strength and a power of the rowing

R. Castro, G. Mujica, and J. Portilla are with the Centro de Electrónica Industrial, Universidad Politécnica de Madrid, 28006 Madrid, Spain (email: {remy.castro, gabriel.mujica, jorge.portilla}@upm.es).

actions can be calculated so as to estimate and compare the rower efficiency with an improvement objective. The specific objectives and contributions of this work can be summarized as follows:

- Design and implementation of an on-board rowing propulsion monitoring system based on a low-cost IoT device, to measure and process precise information of oar movement from the basis of accelerometer, global positioning information and processed data calculation. The device architecture includes wireless communication to connect to a smartphone, so as to provide runtime information to the rower through a real-time monitoring application.
- Analysis and mathematical calculation of the rowing parameters and the proposal of a simplified model to estimate the power of the propulsion, based on the measurements provided by the proposed system, so as to further estimate and compare the outcomes with optimization objectives.
- Design and performance of a comprehensive set of comparative experiments with different rowers and in actual conditions using the implemented system, in order to identify different athlete profiles with the help of the developed device. The characterization of a real load cell has been carried out in order to measure the strength given by the rower as a key parameter for the performance analysis of the athletes' outcomes. The experimental results are supported by the application of automatic strategies to further compare the performance and similarities among the rowers.

The rest of the article is organized as follows: Section II presents the main trends and works in the state of the tart related to the application of IoT for sport training and particular solutions for the rowing sport. Section III is devoted to detail the power calculation analysis and the mathematical aspects to obtain the strength values associated to the rower movement, including a detailed description of the different phases of the rowing propulsion technique. Then, Section IV introduces the overall architecture of the proposed rowing propulsion monitoring system and the description of the specific hardware elements integrated in its design and implementation. In Section V, a complete set of experimental tests with several rowers in real training conditions is presented, and the analysis of the main experimental outcomes are provided based on the data obtained by the proposed system, while in section VI a discussion regarding the experimental results is proposed. Then, section VII explores the application of automatic techniques to further exploit the comparative analysis of the data provided by the IoT system. Finally, conclusions and future work are highlighted in Section VIII.

II. Related Work

The IoT technologies open up a broaden field for professional sport development to increase the physical performance and the optimization/refinement of the techniques [5, 6], as well as in recreational sport to introduce "gamification" or teaching [7]. Usually, within each sport discipline there are specific training equipment to help athletes to improve their techniques and performance. Particularly, in rowing sport there is a common type of static training machine: The ergometer, as shown in [8] or [9, 10]. This tool reproduces water resistance and rowing movement but on the ground, that is, in static conditions. There is no notion of balance or support of the blade, unlike in real water conditions. Nevertheless, it allows acquiring many parameters for the training, such as speed, distance, energy, power and frequency, which are interesting values for a rower.

In rowing, the technique is a crucial point [11] to reach the best performance. Not only frequency and strength have a role in the quality of the propulsion [12], but there are many technical aspects such as the support of the blade in water, movement of the rowers, quality of the catch through complex physic phenomena [13, 14], material behavior [15] or biomechanical behavior of the rower's body [16, 17].

Rowing is a highly spread sport among university students, and is also a very technical discipline using specific materials. For these reasons, there is an important amount of scientific publications related to this activity. Some physic measurement values have been a key point for athletes in their technique improvement. With the development of electronics and sensors, indoor rowing systems started to be equipped with them for data gathering. Since the development and popularization of IT, finer analysis of the rowing movement have been studied and tested, in order to see what was certainly impossible to see in the past. With the miniaturization of the electronic devices and the low price of the sensors, including accelerometers, on-water measurement systems are more and more investigated aiming to study the rower in real conditions of sport training. In [18], a rowing tank is equipped with a strain gauge and a potentiometer. The software part worked on a personal computer and it would be impossible to use this device on water. In [19] the authors present a device able to measure the angular movement and the strength of the oar in the water. It is based on modifying an oarlock which includes a set of strain gauges. The measurements are transmitted to a cellphone or a PC through Bluetooth communication. However, the development of a modified oarlock supposes a strong investment in time and money. In [20], there is a complete study in which a rowing boat is equipped of various sensors to collect the maximum amount of data. The collected data are, for example, the sliding seat movements (measured with a linear potentiometer), the strength given by the athlete, and the weight of the rower on the seat. The riggers have sensors which measure the strength transmitted to water, and the oarlocks have potentiometers in order to measure the angular movement of the oars. In [21], There are acceleration and speed measurements through a device located in the boat shell which transfers the data by a WLAN communication with a computer.

In [22] a three axis accelerometer is implemented on the oar tube with a microcontroller and a Bluetooth module. The main objective is to analyze the synchronization of the movements among the crew, but it also gives a time measurement of the stroke through the accelerometer. The study in [23] is one of the few that focuses on a low-cost device but it only presents

a GPS monitoring. The proposed system aims to have a speed and acceleration reading based on global positioning.

According to the literature, most of the studies aimed to monitor the rowing movement to improve it. However, few are doing it using low-cost highly reusable IoT technologies with the notion of reduced intrusiveness. Among the ones which propose to measure strength and power, most of them are very intrusive or need specific materials [24], so it implies important modifications of the rowing material. This study proposes a new perspective: The developed device must be low-cost, precise, must be able to measure the strength and give access to the power of the rower, and provide on-board real-time information of the data during the on-water rowing training. The device must also be easy to install in any oar or boat and easy to uninstall without any damage of the rowing material, thus maximizing its reusability and adaptability.

In [25] authors propose a very interesting rigid segment combined with quaternion modelling of human body. The work is more intended to provide a biomechanical modeling. However, the sport of rowing presents some differences with kayaking. In fact, the oars in rowing are in motion on the oarlocks and therefore have fewer degrees of freedom. Although monitoring the whole-body movement of rowers is of undeniable interest, in rowing, the differences between two particular strokes and the possibility of a false stance may not be as critical as in kayaking. Instead, the present work is focused on monitoring the rower's movement as an input to the boat + water system dynamics, and therefore it does not target a fine-grained reconstitution of the athlete's body movement. Consequently, the proposed system uses fewer sensors and with significantly lower costs and simplicity of deployment/start-up overall. The measuring and processing system are on board, and it is compact since it is combined with the use of a smartphone, hence simplifying the system implementation and on-site configuration. Furthermore, in [25] the force measurements are not contemplated as in case of the proposed work, where this magnitude is combined with the GPS data provided by the smartphone to feed the runtime analysis with speed and distance values. From the practical application and installation point of view, while wearable devices may be more intrusive to the athlete and may generate certain discomfort (they should be tied to the body), the proposed prototype is implemented on the oar, so it may belong the training material. The advantage is that it can remain on the material between two training sessions or between two different users, so reusability and replicability of the experiments can be performed in a simpler fashion, unlike in the work proposed in [26] where a set of inertial sensors tied to the body are used to model the athlete's movement.

Based on this analysis, while some approaches target a biomechanical analysis of the body movement, the proposed work focuses on immediate and basic values such as speed, distance, strength, power for a runtime self-analysis and a deduction on the relationship between technique (and body movement) and performance (physical values), parameters that can be accessed by the rower during the training session.

Therefore, based on the comparison of the present work with previous existing techniques on water, the intention is not to provide full body tracking as in other works [27]. In this work, the objective is to measure the input given by the athlete in the oar (speed of execution, strength, power) through the device implemented on it, and the response of the system boat + athlete on the water (speed, distance) via the smartphone in the shell. In this way, the athletes can measure with physical magnitudes their action on the oar and compare it with their result (shell speed). They can improve their stroke through readable parameters with the device, for example: force, rhythm, recovery time, ratio of the recovery time compared to the propulsion time, speed of recovery, catch, and release. In addition, our device implements in water a force measurement through a cheap and easy-to-implement way. There is no material modification as in [24] (oar adaptation) or in [19] (oarlock adaptation). From the integration, installation, start-up and on-site usage point of view, the proposed method is comparatively easier to implement, including the manufacturing of the device, and simpler to install and set up. It is also cheaper in terms of sensors (cheaper and a reduced number of units needed) and takes advantage of the smartphone as compilation and processing unit but also as GPS sensor.

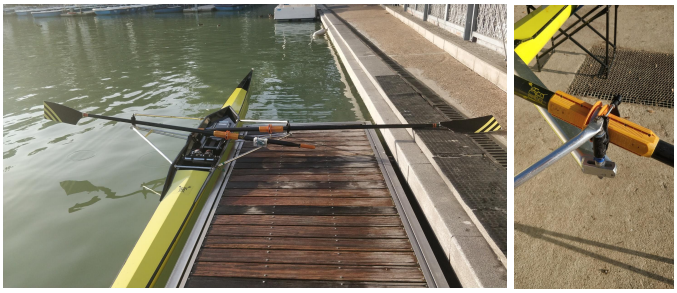

Fig. 1: Olympic rowing boat and its oars, and oarlock.

III. Rowing Power Calculation Analysis

In this section the rowing physic dynamics and the different phases during the technical movement are described, so as to provide a detailed rowing power calculation.

The transmission of rower's strength is allowed by the oar (Figure 1) which acts as a class 2 lever (Fig. 2).

The fulcrum of this lever is the water, the load is the boat and the effort acts on the handle. In the boat referential, the lever rotates around the oarlock's axis. Knowing the rotation speed of the lever and the moment of the strength, we can get the power applied by the rower. Table I depicts the notation used for the power calculation analysis proposed in this section, as well as the description of the parameters used for it. Moreover, in Fig. 3 the representation of the reference frames for the analysis is also shown.

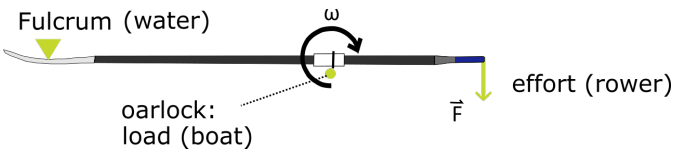

Fig. 2: Oar as a lever.

TABLE I: Used Notations.

Notation	Description
$\frac{d\vec{u}}{dt}\|_R$	Vector $\vec{u}$ derivative respect to the time in the reference frame R.
$\dot{x}$	Function x derivative respect to time.
$\vec{\Omega}_{R_n/R_m}$	Reference frame R_n rotation vector in the reference frame R_m. Its norm is the rotation angular speed of the reference frame R_n in the reference frame R_m (radian per second). Its direction is the rotation axis and its sense depends of the rotation sense using the right hand rule.
$\vec{x} \wedge \vec{y}$	The cross product of the two vectors $\vec{x}$ and $\vec{y}$.
l	Distance between the oar pivot and the device.
θ	Angle between the perpendicular to the shell axis and the main axis of the oar.
$\dot{\theta}$	Derivative of the angle θ respect to time.
φ	Angle between the horizontal and the oar.
v_{boat}	Speed of the boat in the earth reference frame.
R_0	Terrestrial reference frame corresponding to the water or to the riverbank.
R_1	Boat reference frame (the shell of the boat) in rectilinear translation within R_0.
R_2	The reference frame of the oarlock in rotational movement within R_1.

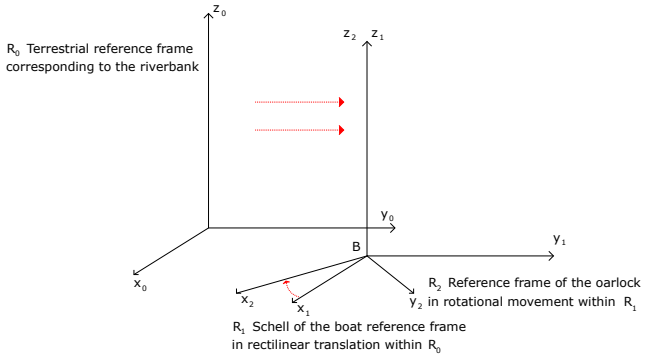

Fig. 3: Reference frames for the rowing power calculation analysis.

The derivative of a vector in a reference frame in movement (non-inertial reference frame) can be calculated with Bour's formula: the derivative of u of the reference frame R_n in movement in the reference frame R_m is:

$$\left.\frac{d\vec{u}}{dt}\right|_{R_m} = \left.\frac{d\vec{u}}{dt}\right|_{R_n} + \vec{\Omega_{R_n/R_m}} \wedge \vec{u}$$

In order to obtain the instantaneous power $P(t) = v(t).F(t)$ and integrate to reach the average power $P(t)$ and the spent energy, we will need $F(t)$ which is the strength function over time, and $v(t)$ which is the speed as a function of the time at the point of the application of the effort (oar's handle). During a typical rowing regatta, boats have very subtle direction changes (rectilinear trajectory). For a limited number of strokes (for example 10) the trajectory can be considered as rectilinear.

The oar has a rotation movement around the oarlock axis in the boat reference frame. Obtaining the rotation velocity of the oar will allow us to calculate the power. For this rotation velocity calculation, an accelerometer (located on the oar's tube) is used to provide runtime data for the power calculation. This data is the acceleration of the oar in the terrestrial reference frame (corresponding to the water or to the riverbank).

The following reference frames are defined:

- R_0, terrestrial reference frame corresponding to the water or to the riverbank.
- R_1, the boat reference frame (the shell of the boat) in rectilinear translation within R_0.
- R_2, the reference frame of the oarlock. This reference frame has a rotational movement within R_1. In this reference frame the oar is assumed as motionless during the propulsive step of the stroke, which is the step studied here. With this hypothesis, R_2 also corresponds to the reference frame of the oar.

All the studied movements occur in the same plane. This plane is perpendicular to the oarlock axis and parallel to the water surface (Fig. 4).

The following reference points are defined (see Fig. 5, 6 and 7):

- O, origin point located in R_0. it corresponds to the departure point of the boat.
- A, point of the boat shell located in the principal axis of the boat.
- B, point of the boat and the oarlock located in the oarlock rotation axis.
- C, point of the oar located on the main axis of the oar (this point is motionless in the oarlock reference frame).
- D, point of the oar where the accelerometer is located (this point is motionless in the oarlock reference frame).
- E, point of the oar where the rower applies the effort (i.e. the handle) (this point is motionless in the oarlock reference frame).

The following basis are defined:

- (O, x_0, y_0, z_0) of the reference frame R_0;
- (B, x_1, y_1, z_1) of the reference frame R_1;
- (B, x_2, y_2, z_2) of the reference frame R_2.

All of these basis are orthonormal and right-handed oriented.

We calculate $\frac{d\vec{OD}}{dt}|_{R_0}$, the point D's speed in R_0 (point where the accelerometer is located). According to the segment addition postulate, we have:

$\vec{OD} = \vec{OA} + \vec{AB} + \vec{BD}$, then:

$$\left.\frac{d\vec{OD}}{dt}\right|_{R_0} = \left.\frac{d\vec{OA}}{dt}\right|_{R_0} + \left.\frac{d\vec{AB}}{dt}\right|_{R_0} + \left.\frac{d\vec{BD}}{dt}\right|_{R_0} \quad (1)$$

A is motionless in the boat, therefore:

$$\left.\frac{d\vec{OA}}{dt}\right|_{R_0} = v_{boat}.\vec{x_0} \quad (2)$$

With v_{boat} as the shell speed in R_0.
R_1 is a non-inertial reference frame, we use the Bour's formula to obtain: $\left.\frac{d\vec{AB}}{dt}\right|_{R_0}$:

$$\left.\frac{d\vec{AB}}{dt}\right|_{R_0} = \left.\frac{d\vec{AB}}{dt}\right|_{R_1} + \vec{\Omega_{R_1/R_0}} \wedge \vec{AB}$$

$$\left.\frac{d\vec{AB}}{dt}\right|_{R_1} = \vec{0} \quad \text{and} \quad \vec{\Omega_{R_1/R_0}} = \vec{0}$$

Since R_1 does not have any rotation movement in R_0 and AB is invariable in R_1, therefore:

$$\left.\frac{d\vec{AB}}{dt}\right|_{R_0} = \vec{0}$$

R_2 being also non inertial:

$$\left.\frac{d\vec{BD}}{dt}\right|_{R_0} = \left.\frac{d\vec{BD}}{dt}\right|_{R_1} + \vec{\Omega_{R_1/R_0}} \wedge \vec{BD}$$

with $\vec{\Omega_{R_1/R_0}} = \vec{0}$, since R_1 does not have any rotation movement in R_0.
Then:

$$\left.\frac{d\vec{BD}}{dt}\right|_{R_0} = \left.\frac{d\vec{BD}}{dt}\right|_{R_1}$$

we calculate now:

$$\left.\frac{d\vec{BD}}{dt}\right|_{R_1} = \left.\frac{d\vec{BD}}{dt}\right|_{R_2} + \vec{\Omega_{R_2/R_1}} \wedge \vec{BD}$$

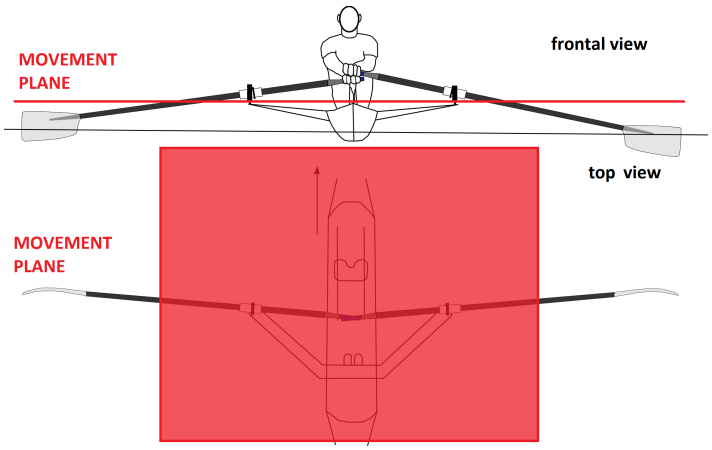

Fig. 4: Movement plane.

$\left.\frac{d\vec{BD}}{dt}\right|_{R_2} = \vec{0}$ because B is a point of the oarlock, D a point of the oar and we consider that the oar is motionless in R_2 during the propulsive step of the stroke.
We know that $\vec{\Omega_{R_2/R_1}} = \dot{\theta}.\vec{z_2}$, because of the definition of the rotation vector.
We can get the coordinate of the vector $\vec{BD}$ projecting in the basis $(B, \vec{x_2}, \vec{y_2}, \vec{z_2})$ (Fig. 8).
with $\vec{BD} = \left|\begin{matrix} +l.\cos\varphi \\ +l.\sin\varphi \\ -d \end{matrix}\right|_{R_2}$ we can calculate the cross product $\vec{\Omega_{R_2/R_1}} \wedge \vec{BD}$:

$$\left|\begin{matrix} 0 \\ 0 \\ \dot{\theta} \end{matrix}\right|_{R_2} \wedge \left|\begin{matrix} +l.\cos\varphi \\ +l.\sin\varphi \\ -d \end{matrix}\right|_{R_2}$$

Therefore:

$$\left.\frac{d\vec{BD}}{dt}\right|_{R_1} = \left|\begin{matrix} -l.\dot{\theta}.\sin\varphi \\ +l.\dot{\theta}.\cos\varphi \\ 0 \end{matrix}\right|_{R_2} \quad (3)$$

In order to use the relation in (3), we project vector: $\left|\begin{matrix} -l.\dot{\theta}.\sin\varphi \\ +l.\dot{\theta}.\cos\varphi \\ 0 \end{matrix}\right|_{R_2}$ into the basis $(B, x1, y1, z1)$:

The projection entails to: $\vec{x_2} = \cos\theta.\vec{x_1} - \sin\theta.\vec{y_1}$ and $\vec{y_2} = \sin\theta.\vec{x_1} + \cos\theta\vec{y_1}$, which allows writing:

$$\left.\frac{d\vec{BD}}{dt}\right|_{R_1} = l.\dot{\theta}.\cos\varphi.(\sin\theta.\vec{x_1} + \cos\theta.\vec{y_1}) - l.\dot{\theta}.\sin\varphi.(\cos\theta.\vec{x_1} - \sin\theta.\vec{y_1})$$

$$\left.\frac{d\vec{BD}}{dt}\right|_{R_1} = l.\dot{\theta}.(\cos\varphi.\sin\theta - \sin\varphi.\cos\theta).\vec{x_1} + l.\dot{\theta}.(\sin\varphi.\sin\theta + \cos\varphi.\cos\theta).\vec{y_1}$$

Simplifying using $\cos(a-b) = \cos a.\sin b - \sin a.\cos b$ and $\sin(a-b) = \sin a.\sin b + \cos a.\cos b$:

$$\left.\frac{d\vec{BD}}{dt}\right|_{R_1} = l.\dot{\theta}.\cos(\varphi-\theta).\vec{x_1} + l.\dot{\theta}.\sin(\varphi-\theta).\vec{y_1}$$

according to the expressions (1), (2) and (3) we obtain,

$$\left.\frac{d\vec{OD}}{dt}\right|_{R_0} = l.\dot{\theta}.\cos(\varphi-\theta).\vec{x_1} + l.\dot{\theta}.\sin(\varphi-\theta).\vec{y_1} + v_{boat}.\vec{y_1}$$

that is, projecting in R_0:

$$\left.\frac{d\vec{OD}}{dt}\right|_{R_0} = l.\dot{\theta}.\cos(\varphi-\theta).(-\vec{y_0}) + l.\dot{\theta}.\sin(\varphi-\theta).\vec{x_0} + v_{boat}.\vec{x_0}$$

Calculating the norm:

$$\left\|\left.\frac{d\vec{OD}}{dt}\right|_{R_1}\right\| = \sqrt{l^2.\dot{\theta}^2.\cos(\varphi-\theta)^2 + (l.\dot{\theta}.\sin(\varphi-\theta) + v_{boat})^2}$$

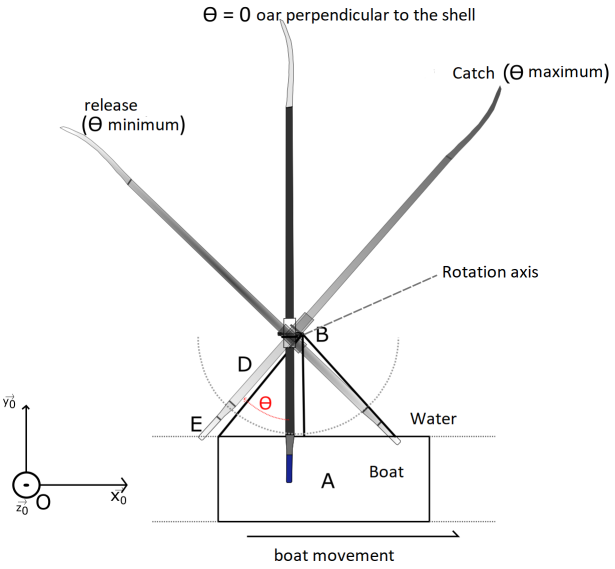

Fig. 5: Reference points in the studied system.

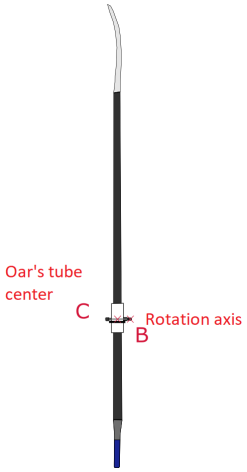

Fig. 6: Detail of the reference points B and C.

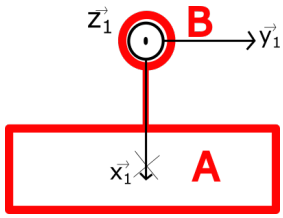

(a) Schematic representation of the boat with the oarlock rotation axis.

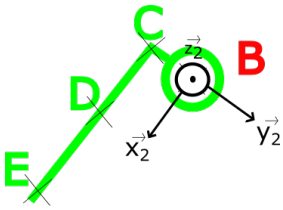

(b) Schematic representation of the oar.

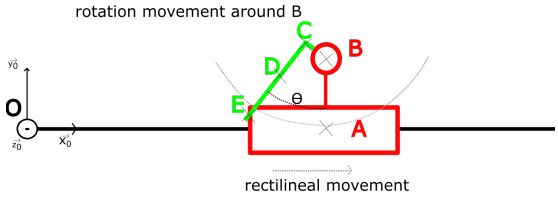

(c) Complete schematic representation of the system (oar+shell).

Fig. 7: Reference system representation.

$$\left\| \frac{d\vec{OD}}{dt}\Big|_{R_1} \right\| = \sqrt{l^2.\dot{\theta}^2.\cos(\varphi-\theta)^2 + l^2.\dot{\theta}^2.\sin(\varphi-\theta)^2 + 2.l.\dot{\theta}.\sin(\varphi-\theta).v_{boat} + v_{boat}^2}$$

For any α we have: $\cos^2\alpha + \sin^2\alpha = 1$, consequently,

$$\left\| \frac{d\vec{OD}}{dt}\Big|_{R_1} \right\| = \sqrt{l^2.\dot{\theta}^2.(\cos(\varphi-\theta)^2 + \sin(\varphi-\theta)^2) + 2.l.\dot{\theta}.\sin(\varphi-\theta).v_{boat} + v_{boat}^2}$$

$$\left\| \frac{d\vec{OD}}{dt}\Big|_{R_1} \right\| = \sqrt{l^2.\dot{\theta}^2 + 2.l.\dot{\theta}.\sin(\varphi-\theta).v_{boat}^2 + v_{boat}^2}$$

Using the square of the expression:

$$\left\| \frac{d\vec{OD}}{dt}\Big|_{R_1} \right\|^2 = l^2.\dot{\theta}^2 + 2.l.\dot{\theta}.\sin(\varphi-\theta).v_{boat} + v_{boat}^2 \quad (4)$$

Where the unknown variables are θ y $\dot{\theta}$.

This is a complex differential equation to resolve especially in real time. Thus, we propose a very simplified model to solve this equation so that a runtime on-board calculation can be performed, from the basis of knowing some extreme values:

a) Dimensions: Taking into account some extreme dimensions that can actually reach a rower on a boat allows delimiting the values within the model, as shown in Fig. 9 and 10.

With these dimensions (see Table II) we can get the φ value, using its sinus.

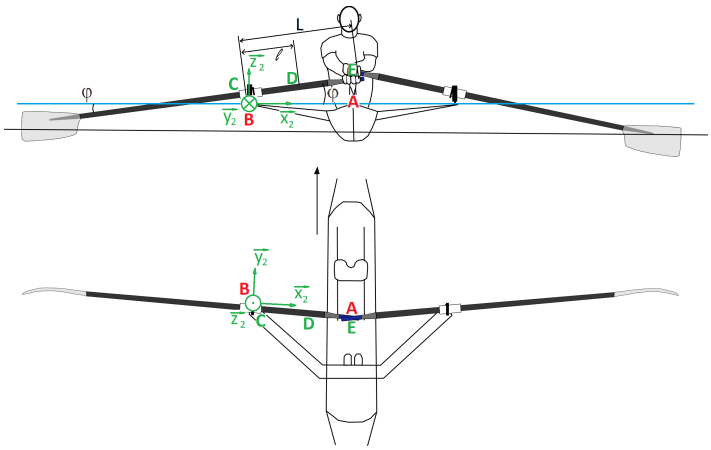

Fig. 8: $\vec{BD}$ projection in the basis $(B, \vec{x_2}, \vec{y_2}, \vec{z_2})$, frontal and top view.

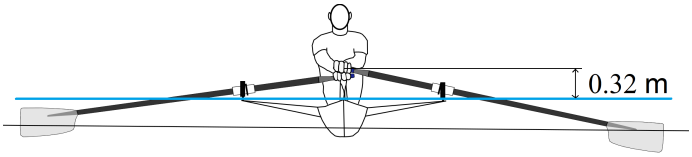

Fig. 9: Characteristic dimensions (front view).

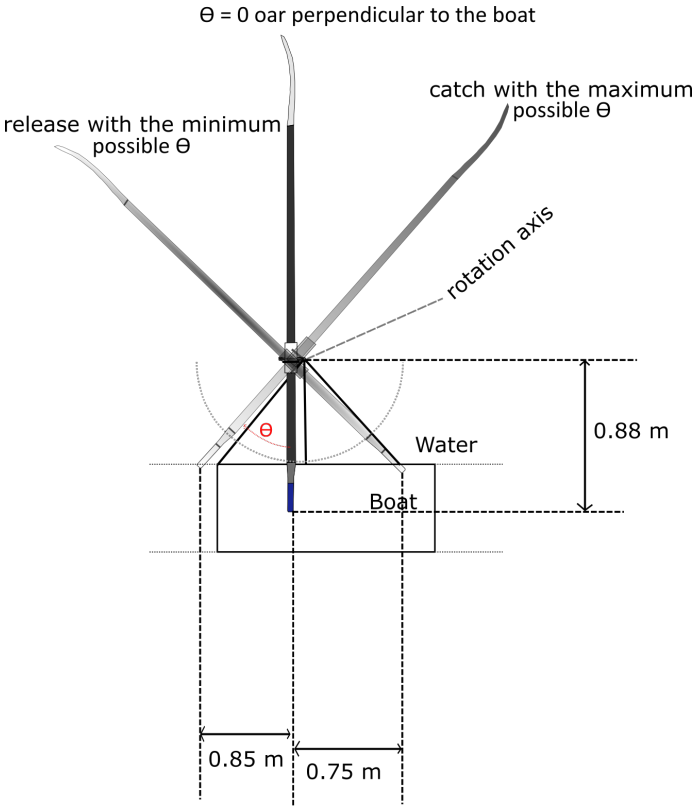

Fig. 10: Characteristic dimensions (top view).

TABLE II: Characteristic dimensions.

Name	Value
L	0.88 m
l	0.33 m
φ	20°

b) Maximum achievable angles: A rower will never attack with an angle θ higher than θ_{max} because they must stretch their arm more than physically possible. Furthermore, they will never release with an angle inferior to θ_{min} (their body put a stop at the back). Therefore, we can conclude from the previous values that the maximum possible angles are the specified in Table III.

TABLE III: θ extreme values.

Name	Value
θ_{max}	45°
θ_{min}	-40°

We can also conclude that $\sin(\varphi - \theta)$ varies between $\sin(20 - 45) = -0.42$ and $\sin(20 - 0) = +0.34$ between an attack with θ_{max} and $\theta = 0$, respectively.
Moreover, we can also say that on the second part of the stroke between $\theta = 0$ and a release with θ_{min}, $\sin(\varphi - \theta)$ varies between $\sin(20 - 0) = +0.34$ and $\sin(20 - (-40)) = +0.87$.

c) Proposed Model: Since we know that $\sin(\varphi - \theta)$ will vary between known limits, we propose the following model:

- On the first part of the stroke $-0.42 < \sin(\varphi - \theta) < 0.34$ we will approximate $\sin(\varphi - \theta)$ equal to its average value between the extreme values, that is, $-0.04 \simeq 0$. Therefore, the expression (4) can be written as:

$$l^2.\dot{\theta}^2 + v_{boat}^2 - \left\| \left. \frac{d\vec{OD}}{dt} \right|_{R_1} \right\|^2 = 0 \qquad (5)$$

  Which is simpler to solve.
- On the second part of the stroke, $0.34 < \sin(\varphi - \theta) < 0.87$, we will approximate $\sin(\varphi - \theta)$ equal to its average value between the extreme values, that is, 0.60. Therefore, the expression (4) can be written as:

$$l^2.\dot{\theta}^2 + 2.l.\dot{\theta}.v_{boat} \times 0.60 + v_{boat}^2 - \left\| \left. \frac{d\vec{OD}}{dt} \right|_{R_1} \right\|^2 = 0 \quad (6)$$

With the expressions (5) and (6), we can obtain the $\dot{\theta}$ value, in radians per second. This value will allow calculating the instantaneous power using F(t) (measured by the sensor) and L, the interior lever of the oar. $P(t) = \dot{\theta}(t)L.F(t)$.

Integrating $P(t)$, we will obtain the average power on a stroke:

$$P_{stroke} = \frac{1}{T}. \int_T P(t).dt$$

where T corresponds to the period of the stroke.

This simplified model is an approximation that is consistent with the real behaviour of the rowing, as detailed in the experimental result analysis.

IV. System Architecture

In Fig. 11 the overall architecture of the proposed IoT system is depicted, with the integration of the main hardware elements that set up the on-board rowing propulsion monitoring system, as well as the Graphical User Interface (GUI) on the on-board mobile device. It is composed of very low cost components, including an accelerometer and a strength sensor for on-board sensing, a Bluetooth module to provide wireless communication between the on-board installed hardware platform and the mobile device, and an embedded microcontroller-based platform to serve as the core of the IoT system to measure, process and transmit the monitoring data in real time, as described in the following paragraphs. Table IV summarizes the main characteristics of the selected hardware components to be integrated with the embedded processing platform.

a) Accelerometer: Accelerometers have been evolved since the first studies of rowing movement analysis, particularly with the MEMS technology. Targeting a very low cost design and integration, the MMA8451Q 3-axis accelerometer [28] has been selected for the prototype.

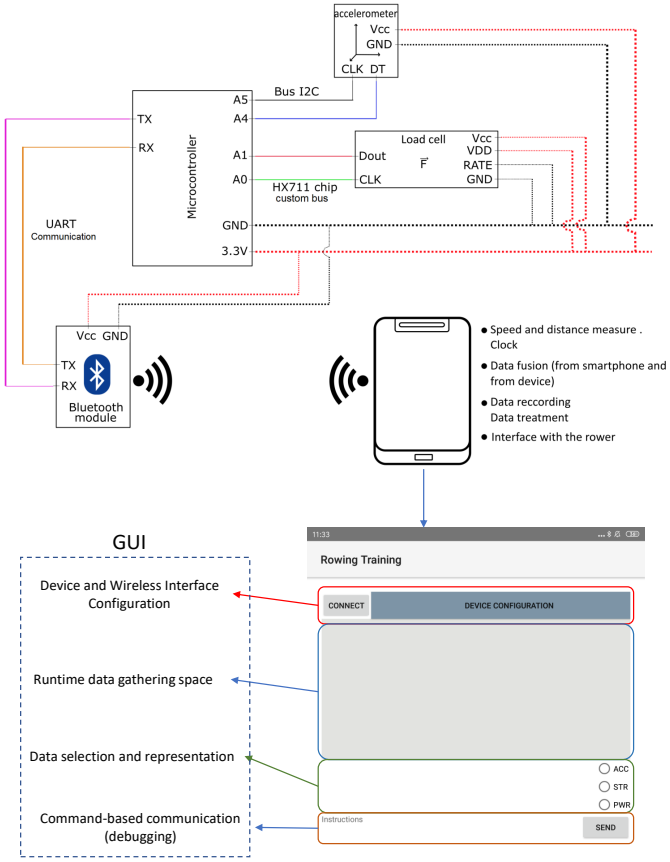

Fig. 11: Overall architecture of the proposed IoT system.

b) Strength sensor: In order to measure the strength given by the rower, the oar's tube deformation will be measured. For that purpose, a load cell normally used for weighting scale will be integrated. the load cell is a metal parallelepiped equipped with two strain gauges mounted in Wheatstone bridge. The advantage of choosing this component is the use of low-cost strain gauges but without the issue of sticking directly the gauge on the surface. Indeed, the load cells have holes that are used with screw and clamping clips for the installation (and it can be remove/replace easily). In this way, any deformation of the oar's tube will entails into a load cell deformation.

To properly treat the input signal from the Wheatstone bridge and supply power to the sensor, the HX711 module from AVIA semiconductor is used [29], which is a very common component used with this type of load cell.

Being a device normally used for weighting scale the standard sampling rate is very low: each measurement is performed every 2 seconds. This is too low for the rowing movement, which lasts approximately 1 second. Nevertheless, the HX711 allows increasing this sampling rate to 80 samples per second, using the on-chip oscillator. This configuration is the one used in this work to perform the on-board sensing.

c) GPS and mobile devices: Seeking a low-cost design of the prototype and taking advantage of the geopositioning modules integrated in today's mobile devices, the GPS location data given by a smartphone will be used, which provides good resolution, ease of use and allows reducing costs on this point. Furthermore, the smartphone serves as the interface between the user and the system, and also performs the data fusion between the device data from the oar and the GPS and timing data from the mobile device. In this way, the processing power, calculation capabilities, storage memory and wireless communication technologies of the smartphone will be exploited in combination with a dedicated embedded platform installed in the rowing boat, thus creating a complete yet easy to integrate IoT on-board monitoring system. For this purpose, an application for Android OS has been developed on *Android Studio SDK*, so that any Android mobile device can be used with this device. In this study a OnePlus 5 smartphone has been used to carry out the experimental tests. Another advantage of the mobile device is a higher capability of data recording and storage, so that it can be further analysed. This is useful for post-processing the rowing sessions by rowers and trainers, and allows carrying out comparative studies to improve particular points in the applied techniques.

d) Bluetooth communication: In order to establish a connection from the oar-located embedded platform and the mobile device, the Bluetooth standard has been selected as the communication technology within the boat, so a local wireless network is created to collect and exchange data between both devices. As described in the following paragraph, the Arduino platform has been chosen as the processing core for the on-board sensing system, so the HC-05 Blouetooth hardware has been used as the communication module. It is a low-cost highly integrated module within the Arduino API.

e) Microcontroller and embedded platform: The strength and acceleration sensors are located on the oar, which have to communicate in a wireless way with the smartphone. For this purpose, an Arduino Duemilanove platform [30] has been selected as the core processing element to gather the measurements coming from the sensors (handling their specific interfaces, and considering the proper sampling frequency), pre-process the data, and then sending it to the smartphone by using the Bluetooth module (through the UART communication interface between the microcontroller and the Bluetooth module). The ease of integration, simplicity and low-cost feature of this platform makes it suitable to serve as the on-oar data collector and sensing manager.

f) On-board smartphone application: The main objective of the application running on the mobile device is to receive the information from the embedded platform trough Bluetooth communication, and then fuse these data with the GPS information from the smartphone. so on one hand it can save the fused data in a recording file for post-processing tasks, and on the other hand represent the information in a GUI for the rower, to follow the evolution and performance of the rowing training in real time. In a second phase, the application will have to produce and display metadata in real time based on the comparison between performance parameters of the rower with respect to an optimization objective. Moreover, the rower will be able to set up several training profiles and configure particular parameters to customize the analysis of a training round.

TABLE IV: Specifications of the selected components.

Model	Manufacturer	Measurement range/feature	Communication/interface
MMA8451Q	NXP	±8g with dynamic selection	I2C
TAL220	Sparkfun	3-200 kg or 30-2000 N	Wheatstone bridge
HX711	Sparkfun	Signal Amplifier	Custom serial bus
HC-05	ITead Studio	Serial Port Bluetooth	UART

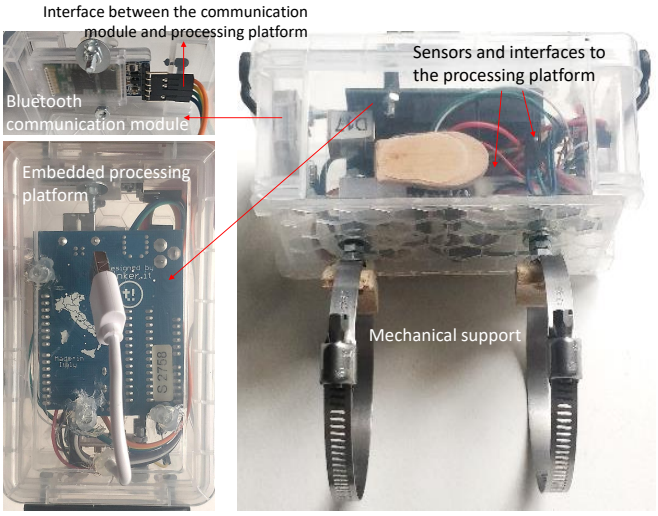

Fig. 12: First prototype of the on-board propulsion monitoring system.

Fig. 12 and 14 show the implementation result of the first prototype for the on-board propulsion monitoring system, with the integration of the hardware elements in a single hermetic commercial box that has been adapted to include the electronic and mechanical components. The total weight of the prototype is 129 g.

V. Experimentation and Results Analysis

A. Characterization and first interpretation

The objective of these first experimental tests is to characterize the rower movement with the maximal precision. The prototype will be always installed in the same place of the oar tube, and with the same orientation.

As represented in Fig. 13 the first sleeve clamp is placed 0.33 m after the rotation axis (between the handle and the rotation axis). A point of reference has been marked on the oar in order to place the prototype in the same way for all experiments, as shown in Fig. 14.

Fig. 13: Representation of the prototype reference distance on the oar's tube.

a) Static experimentation: In order to establish the relation between the oar's tube deformation and the rower's force, an elastic characterization of the oar has been realized. The oar was leaning on the same supports than in the water: fulcrum on the blade and load on the oarlock (see Fig. 15). Different known weights from the handle have been used to emulate a known force of the rower. Then, the deformation has been measured obtaining its relationship with the strength, as depicted in Fig. 16.

The correlation of the linear regression shows a good result, with the trend line representing a pertinent linear model. The points are distributed between the two sides of the straight line. The elastic behaviour of the oar's tube is approved by the experience and $strength = \frac{deformation - c}{k}$ with $c = 41.08$ and $k = 7.70kg^{-1}$.

b) Characterization of the acceleration variations: From the acceleration curves shown in Fig. 17 it can easily be observed the blade preparation at the recovery's end and the blade's rotation at the drive's end. Indeed, spinning the oar's handle, the rower puts in vertical either the z axis (drive) or the y axis (recovery). Thus, the accelerometer will measure the g-force on the z axis (drive) or on the y axis (recovery).

Based on these observations, it is possible to interpret the acceleration curves, as follows:

- During the recovery, the g-force is in the y axis direction. Thus the acceleration value will be approximately -10 $m.s^{-2}$ on the y axis.
- During the drive, the g-force is in the z axis direction. Thus the acceleration value will be approximately -10 $m.s^{-2}$ on the z axis.
- When the acceleration changes from an average value between 0 and 5 to -10 $m.s^{-2}$ on the z axis, it corresponds to the blade preparation before the catch.
- When the acceleration changes from -10 $m.s^{-2}$ to an average value between 0 and 5 $m.s^{-2}$ on the z axis, it corresponds to the blade rotation before the recovery.

With these curves the stroke frequency can also be obtained: 23 strokes per minute in the experimental characterization. Thanks to the acceleration curves the catch and release limits under the stroke cycle can be obtained. Integrating within this interval provides access to the speed of movement of the device and therefore of the oar on the stroke, and then the corresponding movement.

c) Strength: When the blades are in a vertical position, it corresponds to the drive to the catch or to the finish of the stroke. When the blades are in an horizontal position, the recorded strength signal corresponds to parasite movements

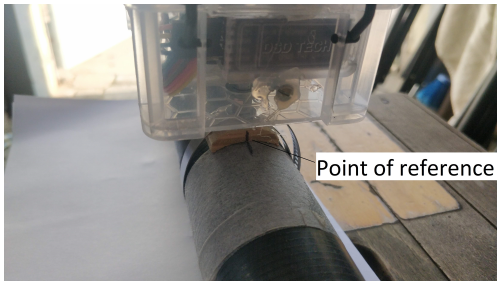

Fig. 14: Point of reference for the device orientation.

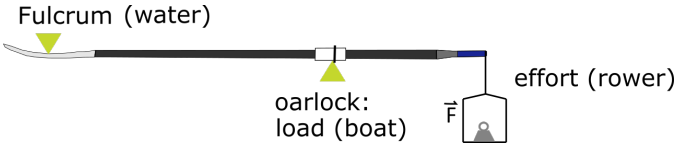

Fig. 15: Representation of the parameters for the static experiment.

or to a flexion of the oar under its own weight, which has no interest here.

Regarding the oar's tube deformation, the higher peaks correspond to the drive phases. It can also be observed little peaks during the recovery phases. These are probably due to an elastic behaviour of the oar's tube when the blade gets out the water: the lever loses its fulcrum and the mechanic pressure vanishes. The tube then goes back to its initial torsion state in an impetuous movement causing this deformation peak.

By treating the torsion signal, the offset signal can be eliminated and the torsion can be translated into a strength based on the relation found during the static experimentation. Moreover, the signal can be filtered when the blade is horizontal (no propulsive phases).

Several features can be highlighted from the treated strength signal (see Fig. 18). The propulsive phase has three distinct steps: A negative strength peak, a higher positive peak, and a third negative peak.

- First negative peak: demonstrates a good technique, the rower introduces its blade in water before the beginning of the drive (before applying strength). Once the blade is in the water and before the propulsion, the water relative movement due to the shell movement acts on the blade and deforms the tube.
- The rise to the maximum strength corresponds to the muscular action of the rower: the increasing part corresponds to the stronger muscles action (legs), the decreasing part corresponds to the weaker muscles (body and arms).
- Sometimes a little negative peak can be observed after the main strength peak: It means that the rower finished the drive (the mechanic pressure disappeared and the oar's tube goes back to its initial state in an impetuous way) but has not put the blade in an horizontal position yet.

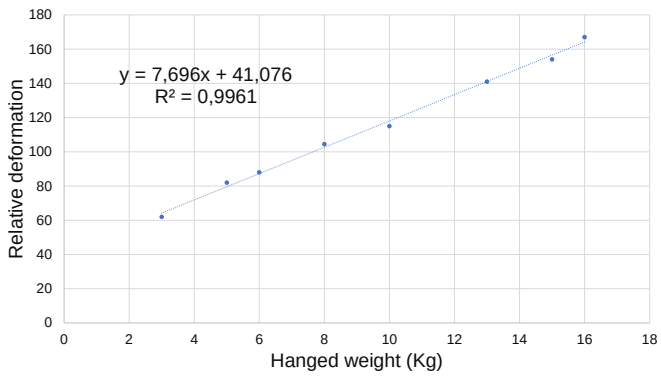

Fig. 16: Deformation as a function of the weight.

To sum up the movement and its characterisation through strength and acceleration signals, Fig. 19 shows the links between curves and the rower position.

d) Sampling frequency: The sensing parameters are measured with a sampling frequency of 11.5 Hz. This value is very higher with respect to the rowing movement frequency. The rowing movement has a frequency between 0.3 Hz and 0.8 Hz as maximum. In this way, a pertinent sampling rate can be assured, avoiding information loss.

B. Comparative experimentation

The IoT rowing propulsion system prototype has been tested on board through a set of rowing training sessions in a real scenario, where 6 different rowers take part on the experiments. Table V presents the main characteristics of the rowers, and the prototype allowed analysing each rowing profile in detail. Each rower has been requested to perform a short route (see Fig. 20) using a single scull (one rower boat). The boat and the oars are the same for all rowers. The experiments took place one after the other at same moment of the day with a constant temperature. Prior to the rowing sessions the device is tested on place to analyze the behavior of the sensing measurements so that possible noise influence can be realized from the actual dynamics of the rowing. This allowed performing on-site hardware and software calibration tasks.

The rowers have all begun the route from the same point, and there is a part of the route to warm up and get familiar with the device. Then, on the last 150 m the data were registered. This is the analysed part in the comparative results. It is also interesting to highlight that some gust of wind until 20 $km.h^{-1}$ may have slowed a bit the rowers. In Fig. 21 a photo of one of the rower in the real training scenario is presented, with the single scull used for the experimental tests.

Based on the information provided by the IoT system, the rowers' training patterns and rowing profiles have been extracted and interpreted, also taking into account the valuable feedback and expertise provided by the rowers and the trainer. Moreover, apart from the technological background of the authors, one of the authors is also a federated athlete of the rowing sport, with experience in regional and national competitions, so his experience in the field is also used to analyzing with deeper details and from a combined technical-sport point of view the progress and results of the experiments.

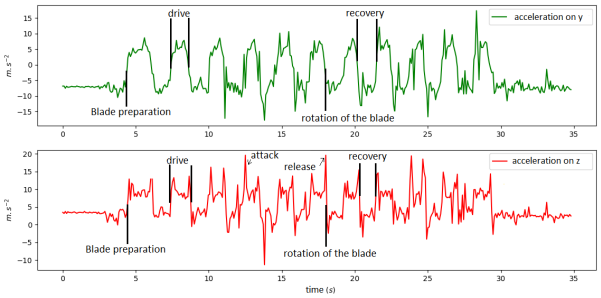

Fig. 17: Experimental acceleration curves.

TABLE V: Characteristics of the rowers for the experiments

Rower	Characteristics
1	Junior with some years of experience, local competitions 70 kg, 1.75 m approximately
2	Junior with some years of experience, local competitions 60 kg, 1.80 m approximately
3	Junior with some years of experience, local competitions 70 kg, 1.80 m approximately
4	Senior with more than 5 years of experience, national competitions 63 kg, 1.75 m
5	Senior with more than 5 years of experience, national competitions 64 kg, 1.75 m
6	Veteran with more than 30 years of experience, national competitions, 75 kg, 1.85 m

1) Rower 1:

a) Accelerations comparison: Fig. 22 shows the results of the acceleration for rower 1, highlighting the main features in the movement. The propulsion seems to have 2 steps, the rower lacks of progressiveness and continuity. During the recovery, there are parasitic movements which demonstrate chocks and friction of the blades on the water. It can be explained by a bad balance of the rower, which causes energetic losses. Progressiveness refers to the rower's ability to apply his or her strength in the water. For an efficient propulsion, the strength should increase during movement without jerking. On the other hand, balance is the equilibrium of the boat and since the rowing boat shells are unstable, during the rowing movement they tend to fall on one or the other size. The athletes must ensure balance with they technique, their own inertia, and their sense of balance.

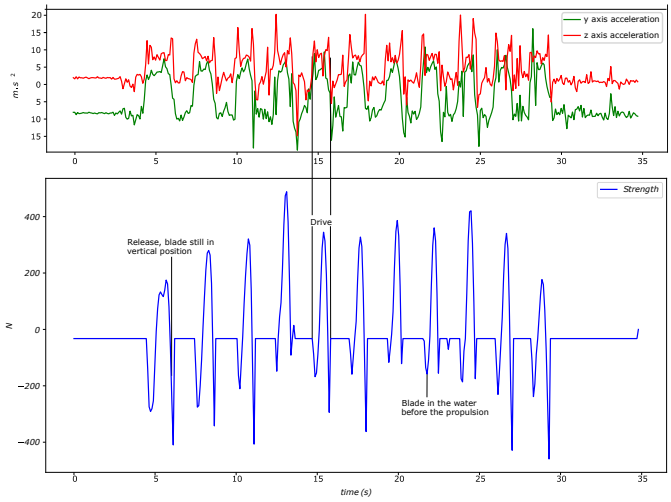

Fig. 18: Experimental strength curve.

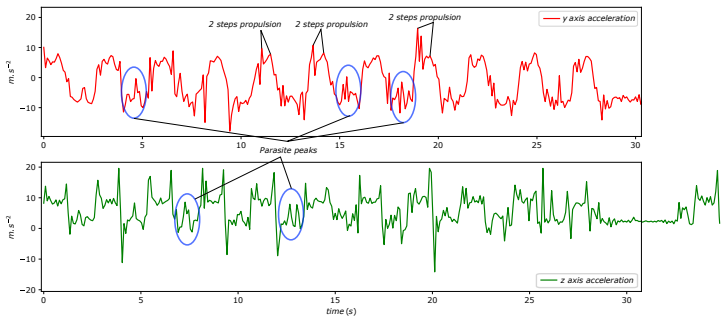

Fig. 22: Acceleration results for rower 1.

b) Strength curves comparison: Fig. 23 shows the performance results regarding the strength measurement for rower 1. It can be highlighted that it corresponds to a strong rower. Peak corresponding to a very prominent release: the rower releases the water in an abrupt way (removing all mechanic constraints) or he maintains his oars in the vertical position during too long time in the air (causing friction with air and a loss of efficiency).

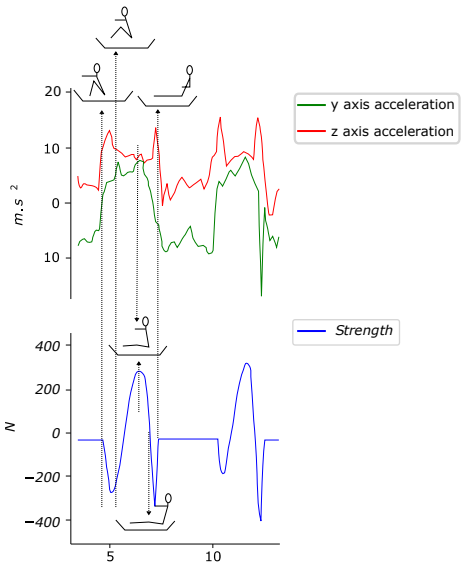

Fig. 19: Links between recorded signals and real movement.

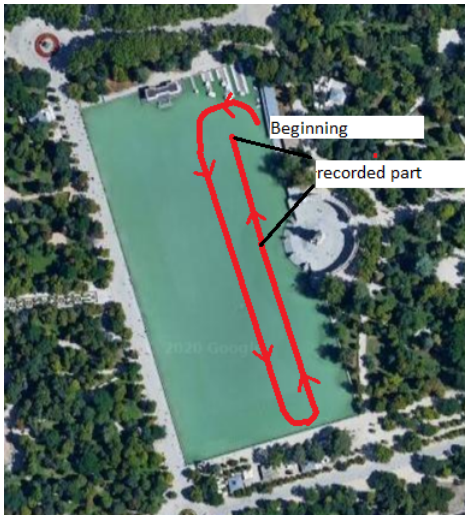

Fig. 20: Representation of the training route used for the experimental tests.

Fig. 21: Rower on the single shull in the real experimental scenario.

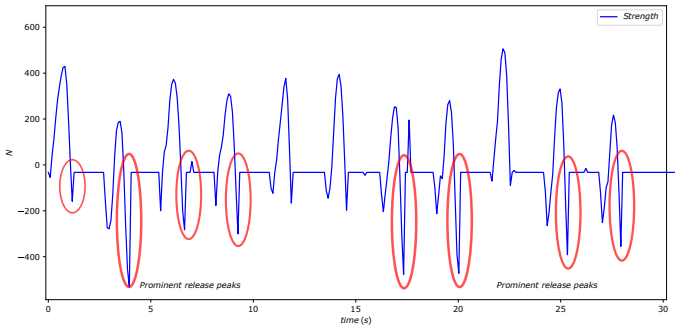

Fig. 23: Strength results for rower 1.

2) Rower 2:

a) Accelerations comparison: Fig. 24 shows a very clea curve during the drive and during the recovery as well, witl no "parasitic signal". The rower 2 has a very progressive driv without irregular movements. During the recovery, there are very little parasitic peaks which demonstrate very little chocks of the blades on the water and a good balance of the rower.

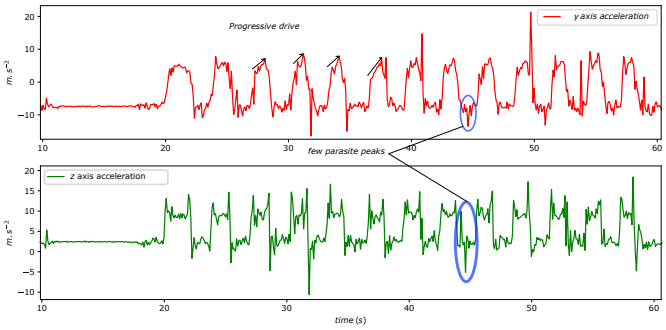

Fig. 24: Acceleration results for rower 2.

b) Strength curves comparison: As shown in Fig. 25, the same particularity during release can be highlighted as in case of the rower 1. This rower applies less strength though.

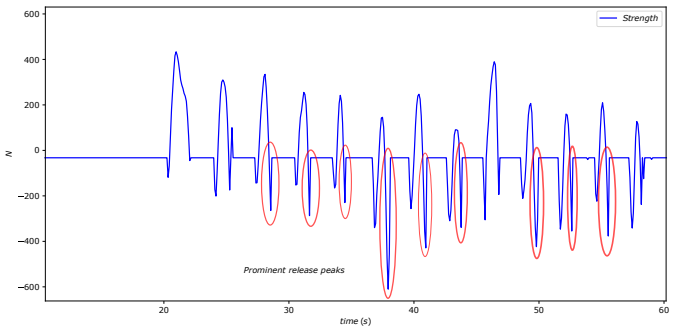

Fig. 25: Strength results for rower 2.

3) Rower 3:

a) Accelerations comparison: Fig. 26 shows little "parasitic signal" pattern, with more intense peaks which corresponds to more hasty movements from the rower.

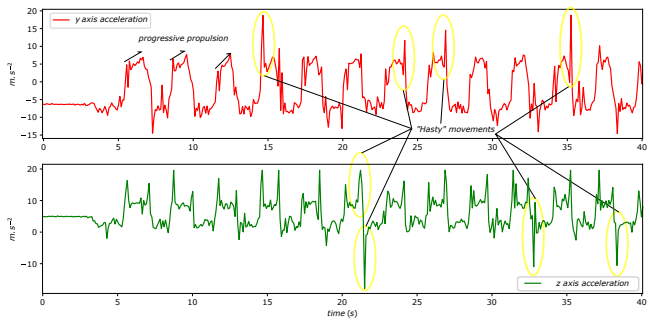

Fig. 26: Acceleration results for rower 3.

b) Strength curves comparison: Rower 3 shows a strength profile similar to rowers 1 and 2 (Fig. 27).

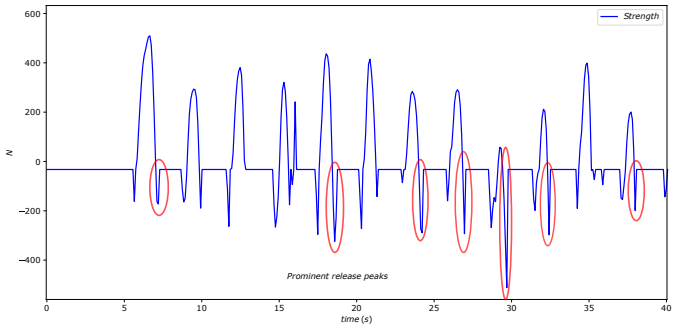

Fig. 27: Strength results for rower 3.

4) Rower 4:

a) Accelerations comparison: Based on the same reasons and interpretations as before, the rower 4 shows a lack of progressiveness during the drive and a lack of balance during the recovery (see Fig. 28.

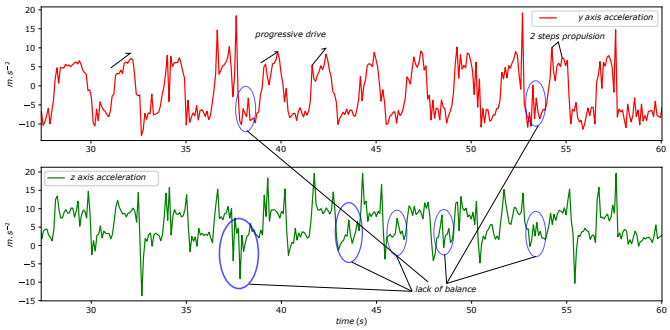

Fig. 28: Acceleration results for rower 4.

b) Strength curves comparison: Results in Fig. 29 shows a more technical and powerful rower (which corresponds to a senior profile in comparison with a junior rower). The catch peaks are less prominent than in the previous cases. The release has also less amplitude than the other rowers. This profile shows a more technical pattern, having more control on its movements.

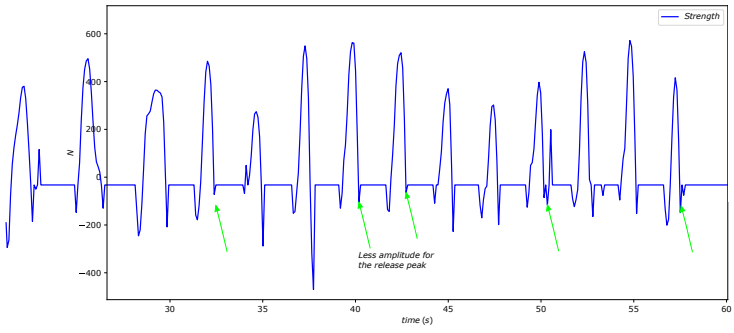

Fig. 29: Strength results for rower 4.

5) Rower 5:

a) Accelerations comparison: Fig. 30 shows a very good drive results for rower 5 (progressively accelerated), although some lack of balance during the recovery.

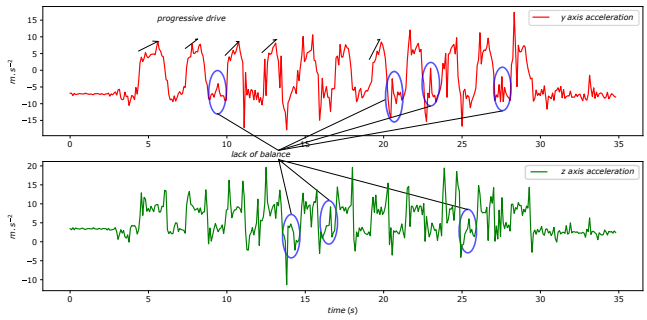

Fig. 30: Acceleration results for rower 5.

b) Strength curves comparison: Similar observations as rowers 1,2,3 about the release but more control on some strokes for rower 5 (Fig. 31).

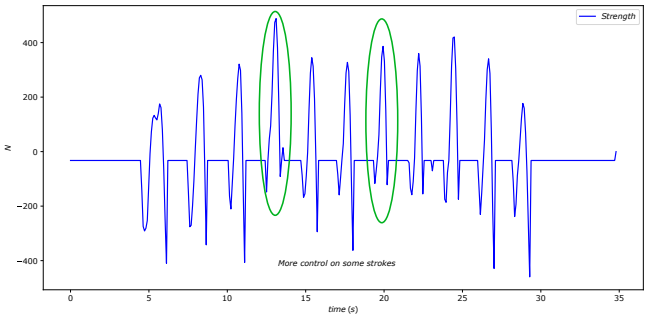

Fig. 31: Strength results for rower 5.

6) Rower 6:

a) Accelerations comparison: As shown in Fig. 32 the rower 6 obtained the clearest signal pattern during the drive after rower 2, and a good balance during recovery. Nevertheless, the drive is not accelerated as it should be.

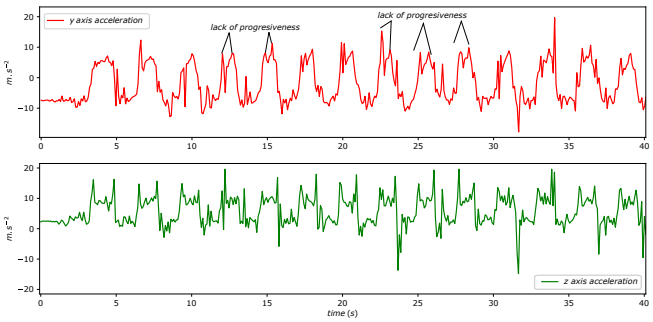

Fig. 32: Acceleration results for rower 6.

b) Strength curves comparison: This rower shows a strength pattern between rower 4 and the rest (Fig. 33). Some strokes are controlled, other contains prominent catches and release peaks. Overall it exhibits a strong rower (compatible with his size and weight).

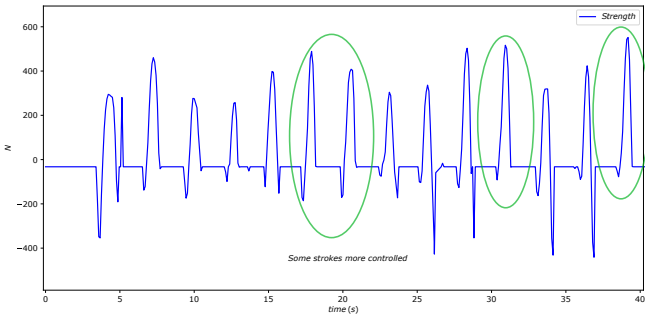

Fig. 33: Strength results for rower 6.

Based on the acceleration outcomes of the different rowers thanks to the data provided by the on-board IoT system, Table VI shows a qualitative summary of the comparative analysis, in accordance with the vertical and horizontal movement of the oars during rowing movement.

TABLE VI: Conclusions on the accelerations performance.

Rower	Highlights and main conclusions
1	Discontinuous drive and lack of balance. These observations are compatible with a junior rower profile.
2	Good balance and progressiveness during the drive. Good level for an inexperienced rower.
3	Hasty movement. Good balance.
4	Lack of balance and peaks during the drive.
5	Good drive but lack of balance during recovery. It could be explained by a lack of single scull practice (boat more difficult in terms of balance).
6	Good balance, correct during propulsion despite a lack of progressiveness.

Based on the strength curves of the different rowers thanks to the data provided by the on-board IoT system, Table VI shows a qualitative summary of the comparative analysis.

TABLE VII: Conclusions on strength performance.

Rower	Highlights and main conclusions
1	Strong rower, abrupt release.
2	Similar to rower 1.
3	Comparable profile to rowers 1 and 2.
4	This rower seems to have more control and more technical performance (in line with the experience).
5	Some strokes with more control.
6	Transitional control level between rowers 4 and 5.

7) Summary of the technical interpretation of the rowers and the comparison of power and speed curves:

a) Rower 1: The balance of this rower can be improved and he needs more control in his movements, however he reaches almost $13km.h^{-1}$ with 22 strokes per minute (see Fig. 34). This rower has room for improvement but his energetic efficiency is very good. All these observations are compatible with a junior rower profile.

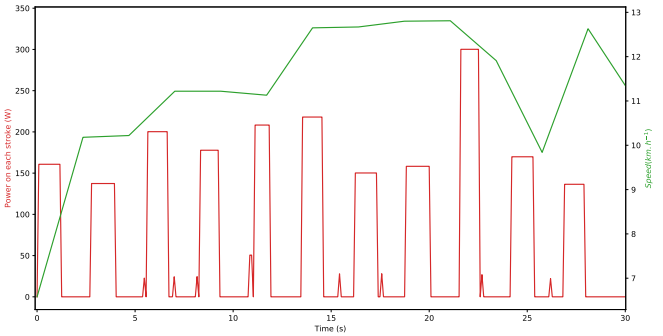

Fig. 34: Speed and power results for rower 1.

b) Rower 2: Rower 2 corresponds to a more powerful rower than rower 1, with a good balance during the recovery. He has a progressive drive but he lacks control in his movement of catch and release. As represented in Fig. 35 he reaches lower speeds than the others but also rows with a lower frequency (19 strokes per minute).

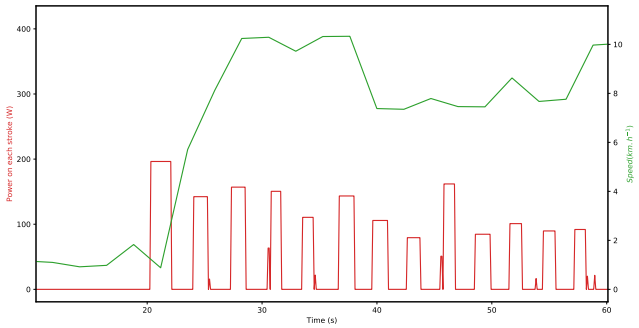

Fig. 35: Speed and power results for rower 2.

c) Rower 3: The technique in release and catch can be improved (more control, softness). Powerful rower who reaches $14km.h^{-1}$ (the fastest) with 21 strokes per minute, as shown in Fig. 36. This speed can be explained by his low weight, for example.

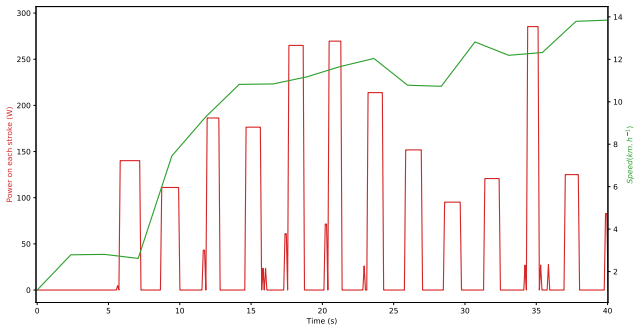

Fig. 36: Speed and power results for rower 3.

d) Rower 4: Technical and powerful rower, with a good performance in terms of speed stability (Fig. 37), although his balance during the recovery penalizes him with friction on the water. Furthermore, his drive shall be more continuous and progressive (accelerated movement). He rowed with a frequency of 24 strokes per minute.

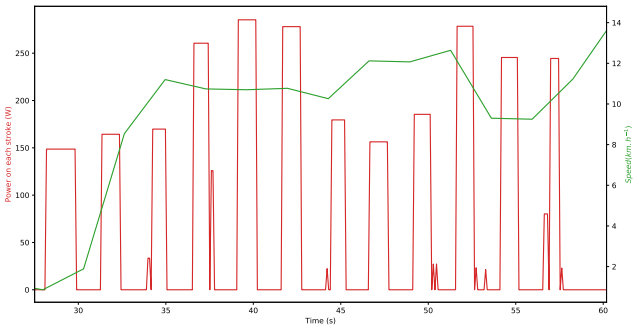

Fig. 37: Speed and power results for rower 4.

e) Rower 5: Rower 5 (Fig. 38) presents a good technical compromise between control on catch and release, and progressiveness of the drive. His balance during the recovery can be improved but he reaches one of the highest speed with a lower power than the others rowers. It can be explained by his low weight and the high frequency (27 strokes per minute).

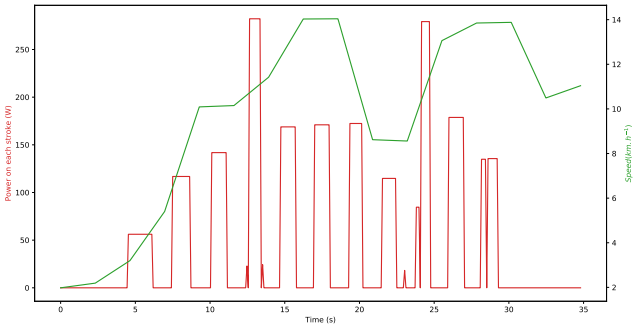

Fig. 38: Speed and power results for rower 5.

f) Rower 6: This rower (Fig. 39) shows a good technical compromise and one of the highest speeds with a lower frequency of 23 strokes per minute.

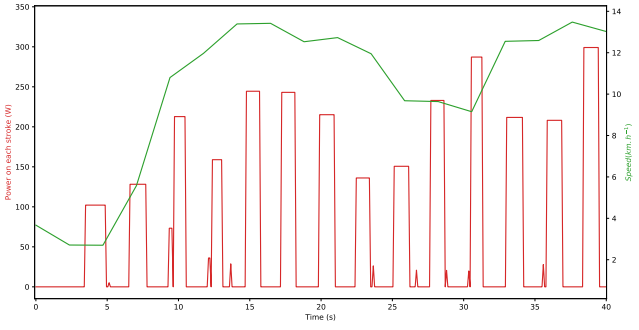

Fig. 39: Speed and power results for rower 6.

VI. Discussion

The implemented system allows an identification of key phases of rowing movement with a good precision and time, and gives an enhanced view for rowers and trainers of the intensity and the quality of the technique. This is performed thanks to the detection of tendencies and the order of magnitudes provided by the IoT device in terms of the studied parameters, particularly regarding the relationship between them and the effective movement (speed) of the boat during training. A direct reading of the speed, the strength, the distance, the time and an estimated value of the power has been obtained based on the proposed on-board IoT monitoring system. The curves as a function of time allow analysing the blades preparation, the blade rotation after release, the vertical and horizontal movements of the blades during recovery and drive. Those are key movements in the sculling technique, which are fields to be improved by any rower.

The observations offered in the experimental analysis here based on these 6 rowers are not absolute: the technique of a rower depends on his or her physical and mental state in the day of the experimentation, on the meteorological conditions, on the material, etc. That can explain why the most experimented rowers can have some downsides (lack of progressiveness, for example). However, the general tendency here is that the more experimented rowers the better the control and efficiency, and they reach higher speeds. Indeed, the device offers the possibility of analysing several key parameters on the dynamics of the training, and they can be combined with other parameters and the experience of the trainers so as to refine the final interpretation and evaluation of the rower performance in a training session.

Regarding the influence of the device on the rowing movement, the 6 participants granted it does not affect the balance of the boat. However, the weight might tend to make easier the preparation of the blade before the catch. For that reason the rower needed a little adaptation time to get used to the device on board.

The power calculation and the speed measurement allow to provide conclusions on the energetic efficiency of the rower, and compare each other to find specific patterns. If a rower reach a higher speed with a lower power, that means that he or she has a better energetic efficiency, which can allow reflecting and distinguishing a better technique.

The interpretations of the acceleration and strength curves characteristics lean on an empirical analysis of rowing movement. This empirical analysis may change based on the rower, the trainer, the time, the country, etc. The quality and value of the proposed device is to provide an objective readability of the rowing movement. Judging if a point is good or bad technique is a subjective action of the training and will depend on the person who reads the data, as in [31]. Anyway, the device provides data related to the real on-water training which can be treated, interpreted and analysed in order to give an technique improvement strategy. To exploit the analysis of the data provided by the IoT system, next section explores the automatic detection and comparison of the different rowers.

VII. Data analysis based on DTW

To further analyze and compare the performance of the rower's behavior, a Dynamic Time Warping (DTW) based analysis of the rowing data has been applied, especially considering the acceleration and strength patterns of the rowers so as to extract similarity and variation features in several scopes: first comparing the outcome curves among the rowers in a DTW cost matrix, and then focusing a comparative analysis

of the deviations between specific rowers with respect to a reference, which is in this case the one with better trade-off between parasitic peaks, speed and balance. Secondly, the comparison applying DTW has been performed considering several rowing windows within a particular rower, which allows analyzing the stability and homogeneity in the rowing technique and their strokes, and how it can impact the result of the propulsion. This also allows extracting conclusions related to what type of improvements can be carried out by the rower in the applied technique, so that the result of the propulsion can be later enhanced.

The DTW is a technique widely used in speech recognition and extended to other application domains [32, 33], including anomaly detection in healthcare context, because of its ability to quantify the differences between signals and identify how the signals differ, even if the signals are not timely synchronized. By detecting the minimum path cost applying matching, insertion and deletion operations to obtain the DTW matrix, a similarity result based on the alignment cost allows quantifying how far or close are two rowing sets, thus providing a magnitude to the performance of the rowing or the window/stroke with respect to the reference. A G Matrix of n x m dimension is computed by applying recursively the expression (7) [34]:

$$G(i,j) = d(x_i, y_j) + min \begin{cases} G(i-1,j) \\ G(i-1,j-1) \\ G(i,j) \end{cases} \quad (7)$$

Where x and y are the signals to be compared, d is the distance between them in points i and j, i = 1 to n, and y = 1 to m, thus the final position $G(n,m)$.

Apart from the acceleration along the y-axis , which corresponds to the axis of the accelerometer that is in the direction of motion during propulsion, the force and a data of the acceleration along the x axis have been also analyzed with DTW. The x-axis is located along the main axis of the oar and measures the acceleration due to the rotation of the oar around the axis of the oarlock. Along this axis, tiny movements of the oar along its axis can also be measured, indicating a bad grip by the rower of the handle. The acceleration along the z-axis is quite similar to the acceleration along the y-axis and its study leads to similar results (same hierarchy of rowers) as the acceleration along y.

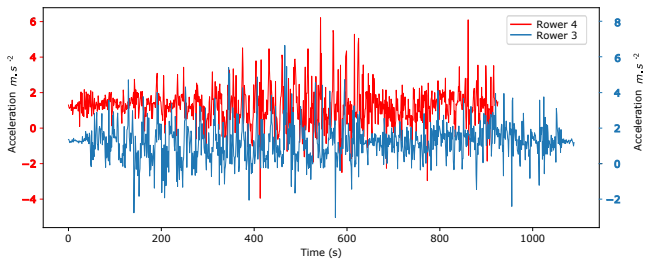

Fig. 40: Acceleration along the x axis for the rowers 4 and 3.

Applied between two rowers, the DTW algorithm allows judging in a quantified way how close two rowers are in their way of rowing. Applied to two signals, here representing the acceleration of rowers 4 and 3 along the x axis, The DTW algorithm provides the alignment cost, the normalized alignment cost as well as the cost matrix. The Normalized alignment Cost (0.2828 in this case) is the alignment cost divided by the total number of values in the two data sets. Figure 40 shows the x-axis acceleration of rowing 3 and 4 respectively, while the graphical representation of the resulted cost matrix applying DTW is shown in Fig. 41.

It then becomes possible to automatically compare rowers with each other on the measured acceleration and force quantities. Tables VIII, IX and X show the normalized alignment costs between each rower for x-axis acceleration, y-axis acceleration and force. This allows comparing all rowers two by two and detect similarities among them. For each rower, the number of points is the same in each data set (acceleration or force). According to the resulted tables, the alignment costs are generally higher for force and lower for accelerations. This means that the rowers are closer together in their acceleration, i.e. in their movement, but apply their force in a much more differentiated way. This is interesting because unlike motion, the application of force is more difficult for an outside observer or trainer to appreciate. This may explain the significant differences between rowers on this data set, apart from the fact that some have more strength than others. The rowers have trained more finely on their movement than on their application of strength.

TABLE VIII: DTW comparison for x-axis acceleration.

	Rower 1	Rower 2	Rower 3	Rower 4	Rower 5	Rower 6
Rower 1	0	1.0695	1.0329	1.0896	1.5589	1.6941
Rower 2	1.0695	0	0.828	0.7812	1.3777	1.5624
Rower 3	1.0329	0.828	0	0.7981	1.254	1.6278
Rower 4	1.0896	0.7812	0.7981	0	1.2989	1.7822
Rower 5	1.5589	1.3777	1.254	1.2989	0	2.63
Rower 6	1.6941	1.5624	1.6278	1.7822	2.63	0

TABLE IX: DTW comparison for y-axis acceleration.

	Rower 1	Rower 2	Rower 3	Rower 4	Rower 5	Rower 6
Rower 1	0	0.3164	0.3424	0.3569	0.4149	0.3573
Rower 2	0.3164	0	0.2454	0.263	0.3292	0.3688
Rower 3	0.3424	0.2454	0	0.2828	0.3641	0.3861
Rower 4	0.3569	0.263	0.2828	0	0.3471	0.4247
Rower 5	0.4149	0.3292	0.3641	0.3471	0	0.753
Rower 6	0.3573	0.3688	0.3861	0.4247	0.753	0

TABLE X: DTW comparison for strength.

	Rower 1	Rower 2	Rower 3	Rower 4	Rower 5	Rower 6
Rower 1	0	18.1627	16.7617	22.6266	27.6510	31.81167
Rower 2	18.1627	0	16.9431	20.7359	28.9902	28.1093
Rower 3	16.7617	16.9431	0	15.5338	23.3671	30.0282
Rower 4	22.6266	20.7359	15.5338	0	31.7684	33.6585
Rower 5	27.6510	28.9902	23.3671	31.7684	0	48.9047
Rower 6	31.81167	28.1093	30.0282	33.6585	48.9047	0

The results of the DTW algorithm are consistent between the different measured quantities. The two most different rowers are always the same (rowers 6 and 5) for the acceleration along the x-axis, the acceleration along the y-axis or for the force curves. The rowers who are closest in their rowing style

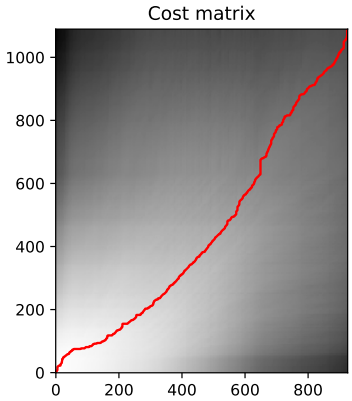

Fig. 41: Normalized DTW cost matrix representation.

do not remain the same, however, if rowers 4 and 2 are closest in terms of acceleration along the x-axis they remain close to each other in terms of the other parameters. The same is true for rowers 3 and 2, and 4 and 3, respectively, who are closer in terms of acceleration along the y-axis and in terms of force.

In general, according to the alignment costs, rowers 1, 2 and 3 are quite close to each other, which is consistent with the fact that they are 3 junior rowers. Rower 4 is senior but very close to rowers 2 and 3 which is not disconcerting given that these categories are close and that the difference in experience between these rowers is not very high. Rower 6 tends to be the most different of all, which corresponds to the fact that he is the only one in the group in his category and with much more experience.

Thanks to the previous analysis of the rowers, they can be compared with a selected reference for each parameter: for the acceleration (y-axis acceleration) Rower 6 was one of the best. It has been found with the automated detection that Rower 1 and 2 are the nearest which is consistent with our previous observation (for rower 2). For strength, the results are less direct. Here the algorithm gives rowers 2 and 3 as the closest to 4. However, the proximity of these rowers may be due to the shape of the peak as the proportion of increasing strength/decreasing strength during the stroke. These criteria are also of interest but more difficult to appreciate from a qualitative point of view by the naked eye. The comparative results of rowers against a model can be even automated below a certain alignment cost (to be defined, for example 0.4 for the acceleration along y-axis), so that it can be affirmed directly that a rower satisfies the model or not for each parameter.

By means of the DTW algorithm the different strokes of the same rower have been compared as shown in Fig. 42 (2 strokes of one rower) and Fig. 43 (DTW cost matrix representation). This comparison can be made iteratively between any stroke and its previous one. A sequence of alignment costs has been obtained for each data set. Table XI shows the average normal alignment cost for each data set of each rower.

This last data processing is particularly interesting in the perspective of on-board or post-training advice to give to the rower as well as to target his strengths and weaknesses. Rowers 2, 3, 4 and 6 should focus their efforts on a more regular application of force while rowers 1 and 2 should

TABLE XI: DTW average results of normalized alignment costs of strokes for each rower.

	Rower 1	Rower 2	Rower 3	Rower 4	Rower 5	Rower 6
x-axis acceleration	0.5766	0.3922	0.4480	0.4119	0.4666	0.4988
y-axis acceleration	2.8244	3.2203	2.4902	2.6799	2.0336	2.7932
Strength	15.383	53.890	63.576	59.391	18.286	68.244

have more regular movements. This analysis also allows a further interpretation of the acceleration along the x axis, which was more difficult to interpret before applying the auto-detection strategy. The acceleration along the x-axis reflects the movement of the oar along its main axis and should also remain similar between the strokes. A good similarity on y-axis acceleration with a lack of similarity on the x-axis acceleration as for rower 4 means a bad catch of the oars with the hand.

Table XI allows identifying the most consistent rowers not in terms of rhythm but in terms of quality of repetition of the same rowing stroke structure. These most consistent rowers are rowers 2, 5 and 1 for x-acceleration, y-acceleration and force respectively. These results are consistent with the final results on power and speed obtained by the rowers. The rowers 1, 2 and 5 reach the best speeds sometimes with the best energy efficiency which is the ultimate guarantee of a quality technique. This result supports the use of the DTW algorithm in the analysis of the results; because it provides more consistence with the findings on the final performance beyond possible prejudices induced by the rowing culture that the observer might have, thus enriching the overall auto-detection plus experience based analysis. As said previously, the technique of the rowers depend on their physical and mental state in the day of the experimentation, on the meteorological conditions, on the material, and so on, and also on the technique instilled by the coaches and their styles. This is why the most experienced rower may not necessarily obtain the best performances and the quality criteria learned in training sometimes hide finer characteristics, difficult to detect but whose variability and influence on the sport of rowing can be appreciated thanks to tools such as the DTW.

VIII. Conclusions and Future Work

Although the proposed implementation is a first-version prototype, it allows a direct and precise reading of strength and acceleration for the rower during the rowing training session. It enables to obtain conclusions about the rowing techniques

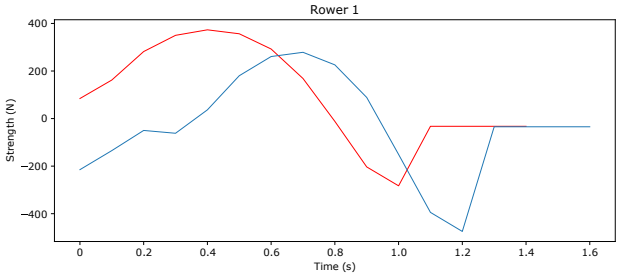

Fig. 42: Comparison of two strokes of rower 1 with DTW algorithm.

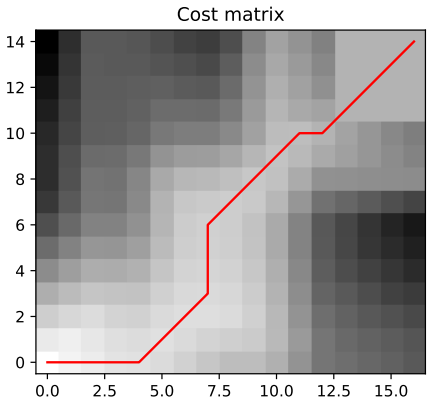

Fig. 43: Normalized DTW cost matrix representation for the stroke comparison.

thanks to an interpretation of the data provided by the IoT rowing monitoring system. This interpretation can be automatized, or it can be performed by a rower or trainer with expertise on the sport (or even a combination of them). The device allows the observation of rowing movement at a hundredth of a second scale, which is difficult for a subjective human eye. Moreover, this study also proposes a power calculation model with the IoT device, which provides coherent results and a direct calculation regardless of the material used (shell oars, rower). Furthermore, this work brings the use of a load cell as a low-cost and easy-to-implement strength sensor for the oar, and the combination of off-the-shelf low-cost technologies is maximized to provide an easy to integrate system. Some future directions are related to refine the shape of the device, reducing its possible impact on rowing sensation (compactness improvement, and optimizing the size and organization of the components), as well as considering the use of energy harvesting techniques based on solar panels to supply power to the on-board device. Moreover, further investigations regarding the inclusion of automatic learning algorithms can be explored to detect hidden features on the rowing movements, so as to complement the feedback provided by the rowers and trainers. Therefore, as a next step within the research roadmap, the application of AI-based analysis can be integrated as a composite toolchain of the training sessions that is fed by the IoT system datasets and rowing features. Finally, the possibility of selecting several profiles will allow customising and adapting the training session to particular optimization objectives for the rowers.

REFERENCES

[1] Philip David Harfield. “Enhancing the mechanical efficiency of skilled rowing through shortened feedback cycles”. PhD thesis. Loughborough University, 2016.

[2] Aimee Mears. “Investigating the effectiveness of digital technology for elite athlete development and support from athlete, coach and support team perspectives”. In: *Final report for the IOC Olympic Studies Centre Advanced Olympic Research Grant Programme 2018/2019 Award* (2019).

[3] J. Portilla et al. “The Extreme Edge at the Bottom of the Internet of Things: A Review”. In: *IEEE Sensors Journal* 19.9 (2019), pp. 3179–3190. DOI: 10.1109/JSEN.2019.2891911.

[4] J. Zornoza et al. “Merging smart wearable devices and wireless mesh networks for collaborative sensing”. In: *2017 32nd Conference on Design of Circuits and Integrated Systems (DCIS)*. 2017, pp. 1–6. DOI: 10.1109/DCIS.2017.8311637.

[5] Mahanth Gowda et al. “Bringing IoT to Sports Analytics”. In: *14th USENIX Symposium on Networked Systems Design and Implementation (NSDI 17)*. Boston, MA: USENIX Association, Mar. 2017, pp. 499–513. ISBN: 978-1-931971-37-9. URL: https://www.usenix.org/conference/nsdi17/technical-sessions/gowda.

[6] Esteban Municio et al. “Continuous Athlete Monitoring in Challenging Cycling Environments using IoT Technologies”. In: *IEEE Internet of Things Journal* 6.6 (2019), pp. 10875–10887.

[7] Á. Tóth and E. Lógó. “The Effect of Gamification in Sport Applications”. In: *2018 9th IEEE International Conference on Cognitive Infocommunications (CogInfoCom)*. 2018, pp. 000069–000074. DOI: 10.1109/CogInfoCom.2018.8639934.

[8] John J Pasierb Jr et al. *Rowing machine with video display*. US Patent 4,674,741. June 1987.

[9] Werner Jonas and Nathanial B Findlay. *Rowing machine*. US Patent 4,880,224. Nov. 1989.

[10] Bojan R Jeremic and Hrayr Nazarian. *Electronically controlled mechanical resistance device for rowing machines*. US Patent 10,307,631. June 2019.

[11] Clara Soper and Patria Anne Hume. “Towards an ideal rowing technique for performance”. In: *Sports Medicine* 34.12 (2004), pp. 825–848.

[12] AH McGregor, AMJ Bull, and R Byng-Maddick. “A comparison of rowing technique at different stroke rates: a description of sequencing, force production and kinematics”. In: *International journal of sports medicine* 25.06 (2004), pp. 465–470.

[13] Chris Pulman. “The physics of rowing”. In: *University of Cambridge: Ithaca* (2005).

[14] Brian Sanderson and Walter Martindale. “Towards optimizing rowing technique”. In: *Medicine and science in sports and exercise* 18.4 (1986), pp. 454–468.

[15] Romain Labbé et al. “Physics of rowing oars”. In: *New Journal of Physics* 21.9 (2019), p. 093050.

[16] Volker Nolte. “Introduction to the biomechanics of rowing”. In: *FISA coach* 2.1 (1991), pp. 1–6.

[17] W Roth et al. “Force-time characteristics of the rowing stroke and corresponding physiological muscle adaptations”. In: *International Journal of Sports Medicine* 14.S 1 (1993), S32–S34.

[18] Jonathon C Henry et al. “An evaluation of instrumented tank rowing for objective assessment of rowing performance”. In: *Journal of sports sciences* 13.3 (1995), pp. 199–206.

[19] Dominik Cirmirakis and John K Pollard. "Rowing optimisation". In: *2009 IEEE International Workshop on Intelligent Data Acquisition and Advanced Computing Systems: Technology and Applications*. IEEE. 2009, pp. 159–161.

[20] Stefano Bettinelli et al. "An Integrated Data Acquisition System for on-Water Measurement of Performance in Rowing". In: *Strain* 46.5 (2010), pp. 493–509.

[21] Klaus Mattes and Nina Schaffert. "New measuring and on water coaching device for rowing". In: *Journal of Human Sport and Exercise* II (2010), pp. 226–239.

[22] Marco Avvenuti, Daniel Cesarini, and Mario GCA Cimino. "Mars, a multi-agent system for assessing rowers' coordination via motion-based stigmergy". In: *Sensors* 13.9 (2013), pp. 12218–12243.

[23] Kefei Zhang et al. "Towards a low-cost, high output rate, real-time gps rowing coaching and training system". In: *Proceedings of the 16th International Technical Meeting of the Satellite Division of The Institute of Navigation (ION GPS/GNSS 2003)*. 2003, pp. 489–498.

[24] Franz Konstantin Fuss et al. "Smart oar blade for hydrodynamic analysis of rowing". In: *Procedia engineering* 147 (2016), pp. 735–740.

[25] Long Liu et al. "Canoeing Motion Tracking and Analysis via Multi-Sensors Fusion". In: *Sensors* 20.7 (2020). ISSN: 1424-8220. DOI: 10.3390/s20072110.

[26] Long Liu et al. "Paddle Stroke Analysis for Kayakers Using Wearable Technologies". In: *Sensors* 21.3 (2021), p. 914.

[27] Paul Noble Page and DA Hawkins. "A real-time biomechanical feedback system for training rowers". In: *Sports Engineering* 6.2 (2003), pp. 67–79.

[28] NXP Semiconductors. "MMA8451Q, 3-axis, 14-bit/8-bit digital accelerometer". URL: https://www.nxp.com/docs/en/data-sheet/MMA8451Q.pdf.

[29] Sparkfun. "Load cell amplifier HX711". URL: https://cdn.sparkfun.com/assets/b/f/5/a/e/hx711F_EN.pdf.

[30] Arduino. "Arduino Duemilanove". URL: https://www.arduino.cc/en/Main/arduinoBoardDuemilanove.

[31] Anton Umek and Anton Kos. "Wearable sensors and smart equipment for feedback in watersports". In: *Procedia Computer Science* 129 (2018), pp. 496–502.

[32] Ryohei Osawa, Takaaki Ishikawa, and Hiroshi Watanabe. "Pitching Motion Matching Based on Pose Similarity Using Dynamic Time Warping". In: *2020 IEEE 9th Global Conference on Consumer Electronics (GCCE)*. 2020, pp. 1–5. DOI: 10.1109/GCCE50665.2020.9291730.

[33] Yang Li et al. "Human Activity Classification Based on Dynamic Time Warping of an On-Body Creeping Wave Signal". In: *IEEE Transactions on Antennas and Propagation* 64.11 (2016), pp. 4901–4905. DOI: 10.1109/TAP.2016.2598199.

[34] Haowen Zhang et al. "Dynamic time warping under product quantization, with applications to time series data similarity search". In: *IEEE Internet of Things Journal* (2021), pp. 1–1. DOI: 10.1109/JIOT.2021.3132017.

Rémy Castro received the General Engineering Degree from École Centrale de Nantes and M.Sc. in Energy Engineering from Universidad Politécnica de Madrid (UPM) in 2018 and 2020, respectively. Prior to that, he enrolled in a 2-year intensive program in Marseille, France, for preparing the national competitive exams to entry French Schools of Engineering, with strong competences in mathematics, physics, and chemistry. He has been actively involved in the practice of the rowing sport, participating in regional and national competitions. He has a strong interest in applying novel technologies to analyze and improve the sport training under real conditions, combining his technical and sport expertise in the field.

Gabriel Mujica (M'18) received the Ph.D. degree in Industrial Electronics engineering from the Universidad Politécnica de Madrid (UPM). He is an Assistant Professor and Research Member in the Center of Industrial Electronics, Universidad Politécnica de Madrid, where he is mainly involved in the area of Internet of Things, Networked Embedded Systems and wireless sensor networks (WSN).

He has participated in different national and European research projects (including Horizon 2020 projects), related to the development and optimization of WSN, as well as the integration of heterogeneous IoT edge hardware, software, and communication technologies for wireless distributed systems, with a particular focus on the performance evaluation and optimization of sensor platforms under real deployment contexts. He has authored several contributions in high-impact conferences and journals. He has collaborated in the organization of research tutorials and seminars, and as a reviewer and guest editor in international conferences and indexed journals. Moreover, his visiting research stay at Trinity College Dublin strengthened the vision and applicability of IoT technologies for smart and sustainable cities, leveraging collaborations in the area of distributed systems within such contexts. Currently, his main research interests are related to multi-hop distributed networks, hardware-software co-design and protocols for IoT embedded systems in smart urban application scenarios.

Jorge Portilla (M'09-SM'18) received the M.Sc. degree in Physics from the Universidad Complutense de Madrid, Madrid, Spain, on 2003, and the Ph.D. degree in Electronic Engineering from Universidad Politécnica de Madrid (UPM), Madrid, Spain, in 2010.

He was a Visiting Researcher with the Industrial Technology Research Institute, Hsinchu, Taiwan, in 2008, and also with the National Taipei University of Technology (Taipei Tech), Taipei, Taiwan, in 2018, working on wireless sensor networks hardware platforms and network clustering techniques. He is currently an Associate Professor with Universidad Politécnica de Madrid. He carries out his research activity within the Centro de Electrónica Industrial, belonging to the UPM. His research interests are focused on wireless sensor networks, Internet of Things, digital embedded systems, and reconfigurable FPGA-based embedded systems. He has participated in more than 30 funded research projects, including European Union FP7 and H2020 projects, and Spain Government funded projects, as well as private industry funded projects, mainly related to wireless sensor networks and Internet of Things. He has numerous publications in prestigious international conferences as well as in journals with impact factor.